Crystal structure of the BAFF–BAFF-R complex and its implications for receptor activation

Ho Min Kim[1], Kyung Sook Yu[2], Mi Eun Lee[3], Dong Ryeol Shin[3], Young Sang Kim[4,5], Sang-Gi Paik[2,5], Ook Joon Yoo[1,6], Hayyoung Lee[5] and Jie-Oh Lee[3]

Published online 25 April 2003; doi:10.1038/nsb925

B-cell activating factor (BAFF) is a key regulator of B-lymphocyte development. Its biological role is mediated by the specific receptors BCMA, TACI and BAFF-R. We have determined the crystal structure of the extracellular domain of BAFF-R bound to BAFF at a resolution of 3.3 Å. The cysteine-rich domain (CRD) of the BAFF-R extracellular domain adopts a β-hairpin structure and binds to the virus-like BAFF cage in a 1:1 molar ratio. The conserved DxL motif of BAFF-R is located on the tip of the β-turn and is indispensable in the binding of BAFF. The crystal structure shows that a unique dimeric contact occurs between the BAFF-R monomers in the virus-like cage complex. The extracellular domain of TACI contains two CRDs, both of which contain the DxL motif. Modeling of TACI–BAFF complex suggests that both CDRs simultaneously interact with the BAFF dimer in the virus-like cage.

BAFF (B-cell activating factor, also termed BLyS, TALL-1, THANK and zTNF4) is a key regulator of B-lymphocyte maturation[1–9]. BAFF-deficient mice fail to accumulate late transitional and mature B cells in their spleens[10,11]. Furthermore, overproduction of BAFF in transgenic mice causes an accumulation of immature and mature B cells and elicits systemic lupus erythematosus (SLE)–like autoimmune diseases[12–15]. Patients with various autoimmune symptoms have elevated levels of BAFF in their sera[14–17]. Intravenous injection of soluble BAFF receptors greatly reduced the symptoms related to these diseases in animal models[10,18–20]. BAFF has sequence and structural similarity with the tumor necrosis factor (TNF) family of proteins, which are involved in immune regulation. BAFF forms hexameric complexes in crystals grown at pH 4.5 and 6.0[21,22] and forms a virus-like cage structure in crystals grown at pH 9.0[23].

Three different receptors, BAFF-R, TACI and BCMA, are capable of binding BAFF[15,18,19,24–27]. The phenotype of mice with an impaired BAFF-R closely resembles that of BAFF-deficient mice. Unexpectedly, TACI seems to have an inhibitory role in B-cell activity[28–30]. TACI-deficient mice have larger germinal centers in their spleens, with more immature and mature B cells. Notably, TACI-null mice were found to be unresponsive to T-cell–independent type 2 antigens, suggesting that TACI is indispensable for this type of immune response. BAFF-R, TACI and BCMA belong to the TNF receptor superfamily[31]. The proteins of the TNF receptor family typically have three or four cysteine-rich domains (CRDs) in their extracellular domains. The canonical CRDs contain six cysteine residues that form three disulfide bridges, stabilizing the elongated antiparallel β-strands[32–37]. BAFF-R is a highly unusual member of the TNF receptor family; it contains one CRD with four cysteine residues, suggesting that the structure and mode of ligand interaction of BAFF-R are substantially different from those of typical TNF receptor family proteins[24,25].

Crystal structure of the BAFF–BAFF-R complex

The structure of the extracellular domain of BAFF-R in complex with BAFF was determined by molecular replacement, using the previously reported BAFF virus-like cage structure as a search probe[23] (Table 1). Although the electron density map was calculated using data limited to a resolution of 3.3 Å, the quality of the map was exceptionally high owing to icosahedral symmetry averaging (Fig. 1*a*). The crystallographic asymmetric unit contains an entire virus-like cage that is composed of 60 BAFF and 60 BAFF-R monomers (Fig. 1*b,c*). Like other TNF family proteins, BAFF monomers consist of a two-layered jellyroll β-sandwich structure. In the BAFF cage complex, two neighboring BAFF trimers make dimeric contact that is mediated by an unusually long DE loop called a 'flap' or 'handshaking' region (Fig. 1*d*)[22,23]. Structural changes in BAFF induced by BAFF-R binding are concentrated near the receptor interaction site, and the overall BAFF structure shows no gross structural changes relative to unbound BAFF.

In the crystal structure, BAFF-R binds to BAFF in a 1:1 molar ratio (Fig. 1*b–d*). The crystallized extracellular domain of BAFF-R is 63 amino acids in length and contains a single CRD (Fig. 2*a,b*). The CRD of BAFF-R spans from Cys19 to Cys35 and forms a short β-hairpin structure. The absolutely conserved DxL motif is located on the tip of the β-turn and is involved in the binding of BAFF (Fig. 2*a,b,* 3*a*). The CRD β-hairpin structure is terminated by two flanking turns made up of residues 20–23 (VPAE) and 35–38 (CGLL). These turn structures are probably stabilized by two disulfide bridges (Fig. 2*a,b*). Residues before Thr17 and after Pro41 are not conserved in TACI or BCMA, and have a highly flexible structure.

Comparison with other TNF receptor family proteins

CRDs of the TNF receptor family are composed of distinct structural modules. Each module type is designated by a letter and by a numeral indicating the number of disulfide bridges[32,34]. Type A

[1]Department of Biological Science, Korea Advanced Institute of Science and Technology, Daejeon, Korea. [2]Department of Biology, Chungnam National University, Daejeon, Korea. [3]Department of Chemistry and School of Molecular Science (BK21), Korea Advanced Institute of Science and Technology, Daejeon, Korea. [4]Department of Biochemistry, Chungnam National University, Daejeon, Korea. [5]Institute of Biotechnology, Chungnam National University, Daejeon, Korea. [6]BioMedical Research Center, Korea Advanced Institute of Science and Technology, Daejeon, Korea.

Correspondence should be addressed to J.-O.L. *e-mail: jieoh@kaist.ac.kr* or H.L. *e-mail: hlee@cnu.ac.kr*

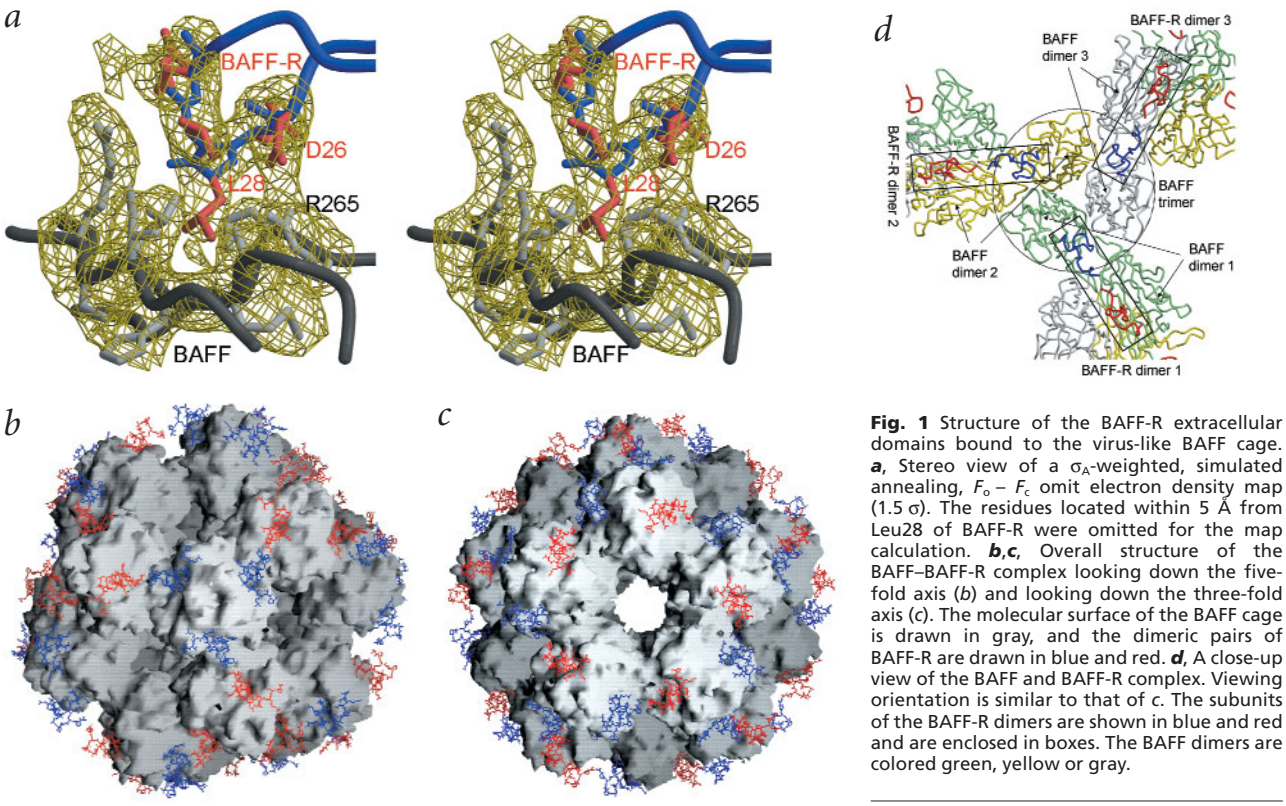

Fig. 1 Structure of the BAFF-R extracellular domains bound to the virus-like BAFF cage. ***a***, Stereo view of a σ_A-weighted, simulated annealing, $F_o - F_c$ omit electron density map (1.5 σ). The residues located within 5 Å from Leu28 of BAFF-R were omitted for the map calculation. ***b***,***c***, Overall structure of the BAFF–BAFF-R complex looking down the five-fold axis (*b*) and looking down the three-fold axis (*c*). The molecular surface of the BAFF cage is drawn in gray, and the dimeric pairs of BAFF-R are drawn in blue and red. ***d***, A close-up view of the BAFF and BAFF-R complex. Viewing orientation is similar to that of *c*. The subunits of the BAFF-R dimers are shown in blue and red and are enclosed in boxes. The BAFF dimers are colored green, yellow or gray.

modules consist of three short β-strands and a disulfide bridge connecting strands 1 and 3. Type B modules also contain three antiparallel β-strands, but the β-strand topologies are different from those of the A modules. The B modules adopt characteristic S-shaped folds reminiscent of paper clips. The topology of the disulfide bridges in the BAFF-R CRD is similar to that of the B2 module. However, the overall structure of the BAFF-R CRD is more closely related to that of the A1 module, rather than the B2 module (see Fig. 4*a*). The BAFF-R CRD structure is readily superimposable with that of the A1 module of TNFR1 CRD3 (r.m.s. deviation = 1.6 Å)[37] and the A1 module of DR5 CRD2 (r.m.s. deviation = 1.3 Å)[35,36]. The structure of the BAFF-R CRD is different from that of the TNFR B2 or DR5 B2 module, and meaningful superimposition is not possible.

The Cys19-Cys32 disulfide bridge of BAFF-R seems to be an essential component of the A1 module of the TNF receptor CRD structures. It is observed in all presently known TNF receptor structures, the TNFR1 and the DR5 structures, and is highly conserved in the sequences of the majority of the TNF receptor family proteins (Fig. 2*b*). In contrast, the Cys24-Cys35 disulfide bridge of BAFF-R is not observed in other TNF receptor structures, and its sequence is not conserved among the TNF receptor family proteins. The Cys24-Cys35 disulfide bridge is probably required to stabilize the A1 module of BAFF-R without a flanking B2 or C2 module. TACI and BCMA have two more cysteine residues in their CRDs. These additional cysteine groups are likely to be involved in the formation of the B2 or C2 modules that may complete the standard TNF receptor CRD structures[32,34]. Our crystal structure of BAFF-R is consistent with the recently published NMR structure of a six-residue synthetic peptide that contains the DxL motif[38].

Asp26 and Leu28 of the DxL motif are the only residues that are completely conserved among BAFF-R-related proteins, except for the structurally important cysteine residues (Fig. 2*b*). Consistent with sequence conservation, Asp26 and Leu28 mediate the most important interactions between BAFF-R and BAFF (Fig. 3*a*). Asp26 of BAFF-R participates in an extensive hydrogen bonding network involving the side chains of Arg265 and Tyr206 of BAFF and backbone atoms of Leu27 and Leu28 of BAFF-R. Notably, the highly conserved Arg265 of BAFF rotates inward by ~90° and forms charge-enhanced hydrogen bonds with Asp26 of BAFF-R. Without a bound receptor, the Arg265 side chain is exposed to solvent and does not interact with the other side chains[21–23]. The conformation of Asp26 of BAFF-R is further stabilized by a hydrogen bond with Tyr206 of BAFF. The conserved Leu28 of BAFF-R binds to a shallow pocket consisting of hydrophobic residues of BAFF: Ile233, Pro264, Leu211 and Ala207. The size and shape of the pocket is complemented by the hydrophobic leucine side chain. The Gly209 residue of BAFF forms the bottom of the Leu28 pocket. This glycine residue is replaced by alanine in TNF-β or valine in TRAIL (Fig. 3*c*). The side chain of the alanine or valine fills up the putative Leu28 pocket, resulting in a flat surface in the TNF-β and TRAIL structures.

In addition to the DxL motif, other residues have supporting roles in the interaction between BAFF and BAFF-R. Val29, Leu37 and Leu38 of BAFF-R and Tyr206 and Leu240 of BAFF form a small hydrophobic interface. This hydrophobic core is generally conserved in the BAFF-R and BAFF family of proteins. However, unlike the Leu28 pocket, the residues involved in this hydrophobic core show substantial sequence variations among the TNF family proteins. Nonspecific and long-range ionic interactions appear to be involved in BAFF-R binding with BAFF. The BAFF receptor binding surface is covered with a large number of negatively charged residues (Fig. 3*b*). Almost all of these acidic residues are conserved in human and mouse BAFF sequences. The negatively charged surface of BAFF complements the positively charged BAFF-R at neutral pH. The interaction is probably nonspecific and long-ranged, because the majority of the basic

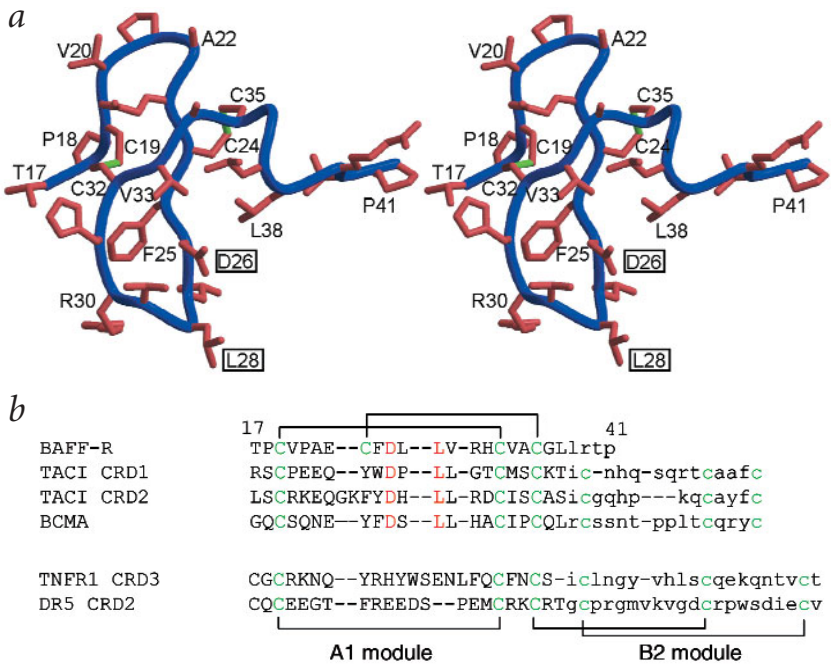

Fig. 2 Structure of the BAFF-R CRD. ***a***, Stereo view of the BAFF-R monomer with the side chains shown in orange. The peptide backbone is schematically drawn as a blue ribbon, with the green lines representing disulfide bridges. The conserved Asp26 and Leu28 residues of the DxL motif are boxed. ***b***, Sequence and structural alignments of BAFF-R-related proteins. The sequences of TACI, BCMA and BAFF-R are aligned (upper). The TNFR1 and DR5 sequences are aligned based on the crystal structures (lower). The cysteine pairs forming the disulfide bridges, as confirmed by the crystal structures, are indicated. The residues given in lower case have limited sequence or structural similarity with BAFF-R and are not aligned. The cysteines are shown in green; the DxL motifs are red.

residues in BAFF-R are located in structurally disordered regions. Notably, the putative receptor binding surface of APRIL, a BAFF-related protein, is positively charged. The charge distribution on APRIL is consistent with the fact that it does not bind BAFF-R[21].

Comparison with other TNF receptor–ligand complexes

The structures of two ligand–receptor complexes of the TNF family, TNF-β–TNFR1 and TRAIL–DR5, have been reported[35–37]. In these structures, the receptors are highly elongated and bind to the crevice between the two neighboring subunits of the trimeric ligand complex. The receptor binding site of the ligand can be divided into two major sites: the A and B patches (Fig. 4*b*). The basal, or B, patch constitutes approximately half of the receptor binding interface of TRAIL and two-thirds of the receptor binding interface of TNF-β. The BAFF B patch, which includes the DE loop, does not participate in the binding interaction with BAFF-R. Instead, it is involved in interactions between adjacent BAFF trimers in the virus-like cage structure. The BAFF DE loop is unusually long and interlocks with the DE loop of the neighboring BAFF trimer (Fig. 4*b*). This type of intertrimeric dimerization is also exhibited in the hexameric BAFF structures of crystals grown at acidic pH[21,22]. The apical, or A, patch of the TNF family of proteins constitutes approximately half of the receptor binding surface of TRAIL and one-third of the receptor binding surface of TNF-β. The BAFF A patch is the sole BAFF-R interaction site.

It is noteworthy that the BAFF–BAFF-R interaction shows considerable differences from the general binding mode of the TNF family of proteins. First, the BAFF A patch is almost completely confined to a single BAFF monomer. In the TRAIL and TNF-β structures, the A patch is divided almost equally between two subunits in the ligand trimer. Second, the β-turn section of the BAFF-R CRD contains the DxL motif and mediates the majority of interactions between BAFF and BAFF-R. In the TRAIL–DR5 and TNF-β–TNFR1 structures, the interactions involving the A patches are mainly mediated by the β-strand portion of the receptor CRD, and the β-turn residues play a relatively minor role. Third, the BAFF-R binding site of BAFF is considerably smaller than those of the other TNF family members. The total buried surface of the BAFF–BAFF-R complex is 922 Å^2, which is approximately half of the total buried surface of the TNF-β–TNFR1 complex and one-third that of the TRAIL–DR5 complex. The smaller interaction surface of the BAFF–BAFF-R complex may provide advantages for the development of small-molecule antagonists, because receptor binding that involves a large interface is often difficult to disrupt using small-molecule drugs.

Ligand-induced trimerization of the intracellular domain is thought to be the major activation mechanism of the TNF receptor family of proteins[31]. A similar trimeric arrangement of receptors is observed in the BAFF–BAFF-R complex (Fig. 1*b–d*). However, the closest interatomic distance between CRDs of the BAFF-R trimer in the receptor–ligand complex is >20 Å, and there are no direct contacts between the CRDs in the BAFF-R trimer. In contrast, the dimeric arrangement between two BAFF-R CRD subunits from neighboring trimers appears to be more intimate (Figs. 1*d*, 3*b*). The shortest interatomic distance between the BAFF-R CRDs in the dimer is 3.8 Å. The BAFF-R dimer is unlikely to be stable without the bound BAFF because the interaction surface between two BAFF-R monomers is very limited and no strong hydrogen or ionic bonds occur between the two monomers. Dimerization can be induced by binding of BAFF-R to either the virus-like BAFF cage or the hexameric BAFF complex. This type of receptor dimerization seems to be unique to the BAFF–BAFF-R complex, because it has not been seen in any other TNF family receptor–ligand complexes. The N- and C-terminal residues outside the conserved BAFF-R CRD have highly flexible structures, and their interatomic spacings between the BAFF-R dimers or trimers are probably not fixed.

Modeling of the TACI–BAFF complex

Structural characterization of the BAFF-R-related proteins TACI and BCMA is important for understanding their physiological roles in BAFF signaling. The TACI extracellular domain contains two CRDs and binds BAFF with nanomolar-range affinity[15]. Notably, the sequence alignment reveals that both the TACI CRDs contain the conserved DxL motifs (Fig. 2*b*). This conservation is unlikely to be trivial, because the sequence homology among BAFF-R-related proteins is relatively low, and, except for the three cysteines involved in the disulfide bridges, DxL motifs are the only residues that are conserved. This conservation suggests that both CRDs may make direct contact with BAFF. To verify this hypothesis, we produced the isolated CRD1 (residues

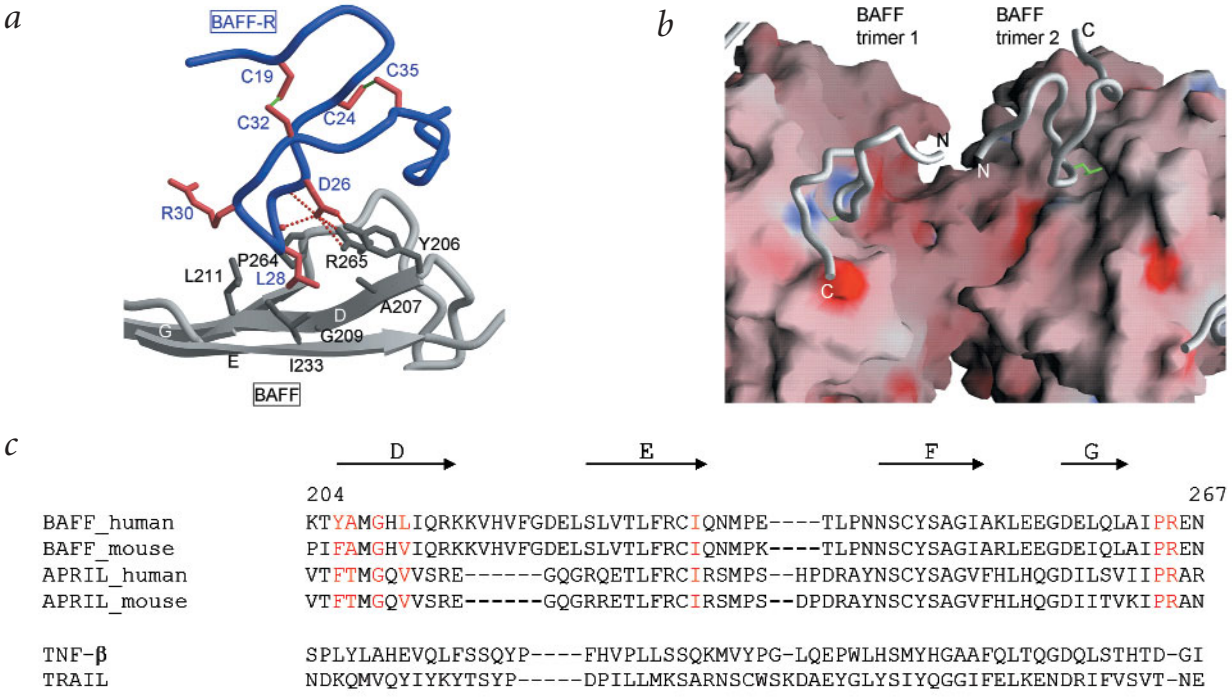

Fig. 3 BAFF-R and BAFF interactions. ***a***, The conserved DxL motif mediating the BAFF-R and BAFF interaction. BAFF is drawn in gray, with the peptide backbone of BAFF-R schematically drawn in blue and the BAFF-R side chains in red. Potential hydrogen bonds are shown as broken lines. The small red ball near Leu28 is the backbone carbonyl oxygen of Leu28. The small gray ball near Gly209 represents the Cα of Gly209. ***b***, Dimeric arrangement of BAFF-R. The BAFF-R CRDs (residues 17–41) are drawn as gray ribbons, with the side chain of the conserved Leu28 residue shown in green. Negatively and positively charged surfaces of BAFF are red and blue, respectively, and the N and C termini of the BAFF-R CRDs are also indicated. ***c***, Residues important for the binding to BAFF-R. The sequences of BAFF, APRIL, TNF-β and TRAIL are aligned. APRIL is the most closely related member to BAFF in the TNF family. Residues that directly interact with the conserved DxL motifs in BAFF-R are indicated in red. The locations of the β-strands are indicated as arrows drawn above the sequences.

14–69) and CRD2 (residues 67–111) of TACI, and determined their binding capabilities to BAFF. Consistent with our model, both CRDs that were tagged with the immunoglobulin Fc domain formed stable complexes with BAFF in pull-down assays (Fig. 5*a*). Under the same experimental conditions, CRDs with mutated DxL motifs did not bind to BAFF (Fig. 5*a*). Furthermore, complete disruption of BAFF binding requires simultaneous mutation of both DxL motifs of the full-length TACI extracellular domain (Fig. 5*b*). In our structure, Arg265 of BAFF mediates the interaction with Asp26 of the BAFF-R DxL motif. Notably, an R265A mutation of BAFF abolished binding of both CRDs (Fig. 5*c*, lanes 3–5), suggesting that the two CRDs of TACI share the same binding site in BAFF. For this binding experiment, an R265A mutant with the BAFF ΔDE background was used because we could not produce sufficient quantities of the R265A mutant with the wild-type BAFF. The BAFF ΔDE mutant has a deletion of the DE loop that mediates formation of the virus-like cage of BAFF[23] background. BAFF ΔDE mutant and wild-type BAFF have binding affinities comparable to those of TACI and BCMA (Fig. 5*c*, lanes 1 and 2)[23]. In the R265A mutant, the Leu28 binding pocket of BAFF is intact (Fig. 2*a*), which may explain the weak binding affinity of the R265A mutant to wild-type TACI through accumulation of two partially disrupted DxL interactions (Fig. 5*c*, lane 3). Initially, these observations were puzzling because we could not clearly explain the simulta-

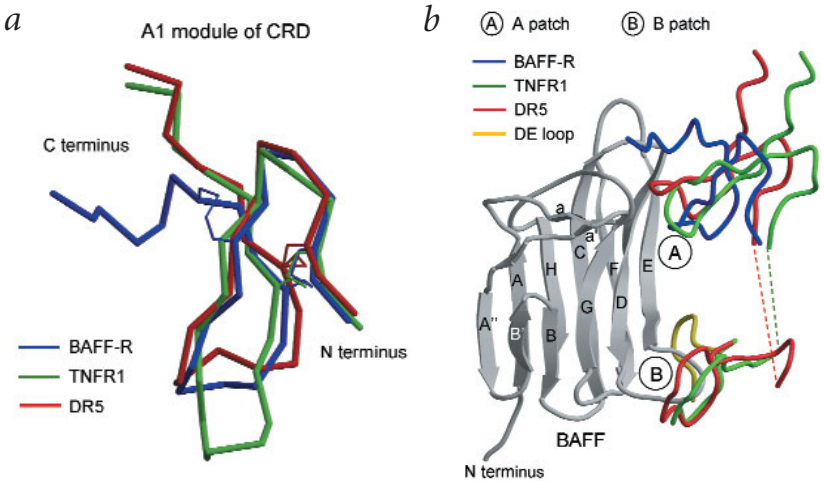

Fig. 4 Comparison of the structures of the TNF-receptor family CRDs. ***a***, The Cα traces of the A1 modules of BAFF-R, TNFR1 CRD3 and DR-5 CRD2 are aligned, with the disulfide bridges shown as thinner lines. The view is rotated by ~180° along the vertical axis of Fig. 2*a*. ***b***, Comparison of the receptor binding sites. The receptors are drawn after aligning the BAFF–BAFF-R, TNF–TNFR1 and TRAIL–DR5 structures. The BAFF structure is indicated schematically (gray). Patches A and B, which are critical for receptor binding, are indicated. The DE loop (residues 217–224) from the neighboring BAFF trimer, drawn in yellow, occupies patch B and mediates the intertrimeric BAFF dimerization.

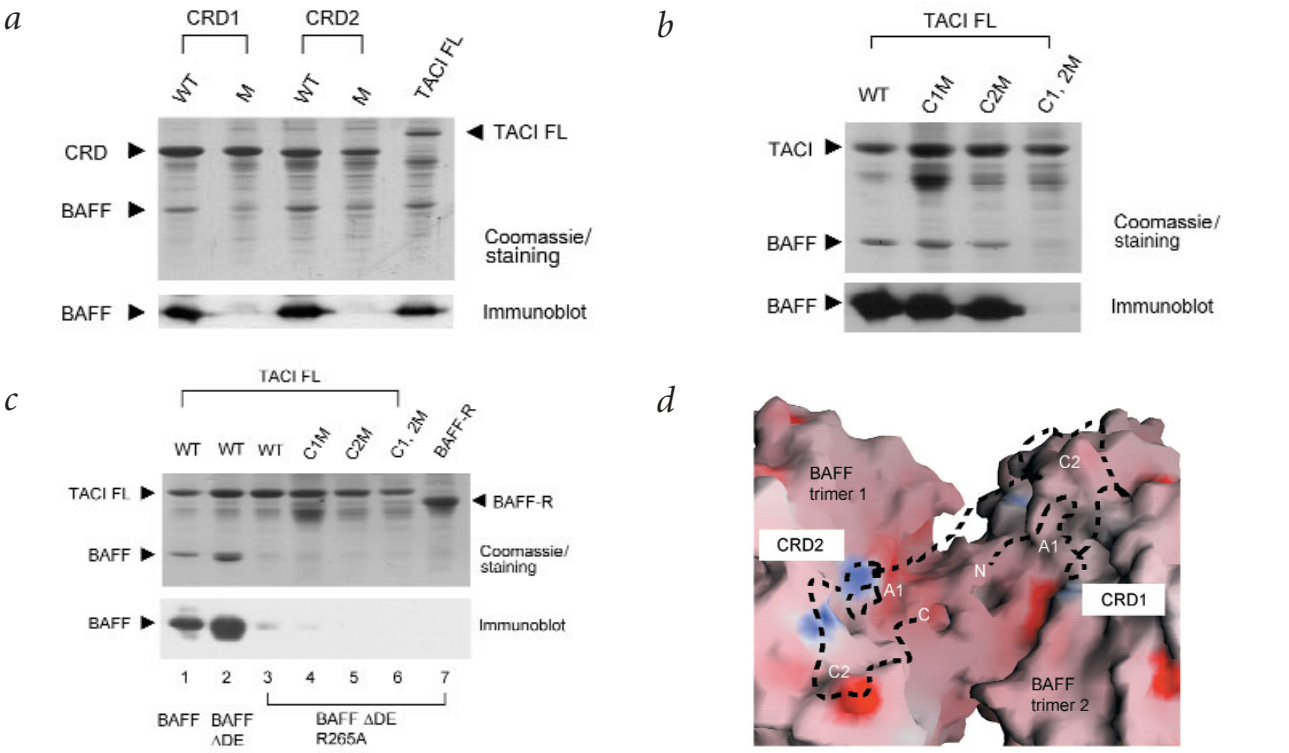

Fig. 5 Characterization of the BAFF and TACI interaction. ***a***, Binding of TACI CRD1 (residues 14–69) and CRD2 (residues 67–111) to BAFF. The conserved Asp and Leu residues of the DxL motifs are mutated to alanines in the mutants (M). The TACI FL is the extracellular domain (residues 1–156) of the full-length TACI. After the binding assay, the resulting duplicate SDS-PAGE gels were visualized either by Coomassie staining or by immunoblot analysis using a polyclonal antibody specific to BAFF (Upstate Biotech) (see Methods). ***b***, Interaction of the TACI CRDs with BAFF. C1M contains mutations of Asp41 and Leu43 of the first DxL motif to alanines. C2M contains mutations of Asp80 and Leu82 of the second DxL motif to alanines. C1,2M contains simultaneous double alanine mutations of both DxL motifs of TACI FL. The resulting duplicate SDS-PAGE gels were visualized as in *a*. ***c***, CRD1 and CRD2 share the same binding site as BAFF. BAFF ΔDE has a deletion of the DE loop. The R265A BAFF ΔDE mutant has a mutation of Arg265 to alanine and a deletion of the DE loop. C1M, C2M and C1,2M are TACI mutants, as described in *b*. The resulting duplicate SDS-PAGE gels were visualized as in *a*. The flexible His_6 tag of the BAFF ΔDE mutant was partially digested during purification and runs as a diffuse band in the SDS-PAGE gel. ***d***, Model of the TACI extracellular domain bound to BAFF. The TACI extracellular domain (residues 32–104) is shown in a broken black line. Negatively and positively charged surfaces of BAFF are colored red and blue, respectively. The N and C termini of the TACI extracellular domain are indicated. Viewing orientation is similar to that of Fig. 3*b*. A1 and C2 modules of CRDs are indicated. The structures of the A1 modules were built with that of BAFF-R CRD as a template. The structures of the C2 modules and the angles between the A1 and C2 modules were adopted from the structure of TNFR1 CRD4 for model building. The molecular modeling was carried out using WHATIF[43].

neous binding of two CRDs of TACI to a single binding site of BAFF. However, careful inspection of the structure reveals that the two receptor binding sites of the BAFF-R dimers in the virus-like cage are close enough to be connected by a suitable linker (Fig. 1*b–d*).

To explain our mutagenesis data, we built a model of the TACI extracellular domain bound to the BAFF complex. In our model, TACI CRDs adopt A1–C2 module structures and simultaneously interact with the BAFF dimer (Fig. 5*d*). The N-terminal half of the TACI and BCMA CRDs has clear sequence similarity with BAFF-R (Fig. 2*b*), and it is likely that this part of the TACI and BCMA CRDs adopts an A1 module structure, similar to that of the BAFF-R CRD. The structural prediction of the C-terminal half of the TACI and BCMA CRDs is less straightforward, because these do not have an obvious sequence similarity with BAFF-R or with other TNF receptor family members whose structures are known. The structures of the C-terminal half of the TNF receptor CRDs can be categorized into two types — B2 or C2 modules — with different disulfide patterns[32,34]. Based on the amino acid spacing between the conserved cysteine residues, Madry *et al.*[39] predicted that the TACI CRDs would have an A1–C2 module structure. The spacing between the terminal cysteine pairs of the known B2 module structure is strictly conserved in the TNF receptor family proteins, where at least seven amino acid residues seem to be required (Fig. 2*b*). The spacing between the final cysteine pair of the TACI and BCMA CRDs is three amino acids long, and this short intercysteine spacing cannot fit into the A1–B2 module combination. Our model, based on the crystal structure and the mutagenesis data, supports the prediction of Madry *et al.*[39] (Fig. 5*d*). When we position the A1 portions of the TACI CRDs in the BAFF-R binding sites of BAFF, the two TACI CRDs cannot be connected with A1–B2 module structures. Because the angles between the A1 and B2 modules show limited variations in the known TNF receptor structures, the B2 module of CRD1 would point in the wrong direction from the A1 module of CRD2, and a linker substantially longer than the natural linker would be required to connect the two TACI CRDs. With the A1–C2 model, the TACI CRDs could be connected by the short native linker that exists between the domains (Fig. 5*d*). Although we can propose a structural model for the TACI CRDs bound to the BAFF dimer, we cannot provide a clear view of the overall structure of the TACI and BAFF complex. It appears that TACI with two CRDs is a potent crosslinking agent for BAFF *in vitro*. Mixing of purified TACI with trimeric or cage complex of BAFF results in immediate precipitation, which makes it difficult to obtain homogeneous samples for biochemical analysis (data not shown). The TACI and BAFF complex may adopt a crosslinked virus-like cage structure or may

Table 1 Data collection and refinement statistics

Space group	$P2_1$
Cell dimensions	
a = 175.5 Å	
b = 194.8 Å	
c = 274.4 Å	
β = 93.3°	
Resolution (Å)	20.0–3.3
Number of reflections	
Total	1,448,322
Unique	280,519
Completeness (%)[1]	93.4 (87.3)
R_{merge} (%)[1,2]	10.8 (26.2)
I / σ[1]	6.9 (1.9)
Number of molecules in asymmetric unit	
Protein	120 (60 BAFF, 60 BAFF-R)
Solvent	0
Metal	40
R_{free} (%)[3,4]	24.8
R_{cryst} (%)[3,4]	23.9
Average *B*-factor (Å^2)	43.8
R.m.s. deviation from ideal values	
Bond lengths (Å)	0.010
Bond angles (°)	1.60
NCS related atoms (Å)	0.034
B-factor (bonded atoms)	1.51
Ramachandran plot	
Most favored (%)	95
Additionally allowed (%)	2.4
Generously allowed (%)	2.6
Disallowed (%)	0

[1]Values in parentheses correspond to the highest resolution shell.
[2]$R_{merge} = \Sigma_{hkl} \Sigma_j |I_j(hkl) - \langle I(hkl)\rangle| / \Sigma_{hkl} \Sigma_j |I_j(hkl)|$, where $I_j(hkl)$ and $\langle I(hkl)\rangle$ are the intensity of measurement *j* and the mean intensity for the reflection with indices *hkl*, respectively.
[3]$R_{cryst,free} = \Sigma_{hkl} ||F_c(hkl)| - |F_o(hkl)|| / \Sigma_{hkl} |F_o|$, where the crystallographic and R_{free}-factors are calculated including and excluding refined reflections, respectively. The free reflections constituted 5% of the total number of reflections.
[4]$|F| > 0\ \sigma$.

form complicated heterogeneous networks of BAFF trimers crosslinked by TACI. In our model, receptor dimerization is not possible in the TACI and BAFF complex because a single TACI molecule interacts with two BAFF subunits. Further experiments are required to show whether a different arrangement of the receptors acts in BAFF signaling.

Conclusions

We present the first crystal structure of the complex formed between BAFF and BAFF-R, showing a novel structural arrangement of the receptors and ligands. Our structural studies provide new insights into BAFF signaling and may help in the development of small-molecule drugs that have pharmacological properties superior to those of protein-based BAFF antagonists.

Methods

Protein expression and purification. The extracellular domain of human BAFF-R (residues 1–63) fused to the Fc domain of human immunoglobulin G1 were coexpressed with human BAFF (residues 134–285) in Hi5 insect cells (Invitrogen) using a recombinant baculovirus system (PharMingen). The secreted BAFF–BAFF-R complex was purified using protein A Sepharose (Amersham Pharmacia Biotech) affinity chromatography. The Fc tag of the fusion protein was removed by thrombin digestion at 4 °C. The cleaved BAFF–BAFF-R complexes were further purified using Source 15S cation exchange chromatography and Superdex-200 gel filtration chromatography (Amersham Pharmacia Biotech). The heterohexameric fractions from the gel filtration chromatography were pooled and concentrated to ~1.0 mg ml^{-1} for crystallization.

Crystallization and data collection. Crystals were grown at 4 °C using the hanging-drop vapor diffusion method by mixing 2 μl of the protein solution and 2 μl of crystallization buffer containing 2.8 M sodium formate, 5% (v/v) ethylene glycol and 100 mM sodium citrate (pH 5.5). Crystals suitable for diffraction experiments grew within 2 weeks. The diffraction data were collected using crystals that were flash-frozen at –170 °C in the crystallization buffer supplemented with 6 M sodium formate at the BL41XL beamline of Spring-8 in Harima, Japan. The crystals belonged to space group $P2_1$ with *a* = 175.5 Å, *b* = 194.8 Å, *c* = 274.4 Å and β = 93.3°. The diffraction data were processed using DENZO and SCALEPACK[40]. The data were 93.4% complete in the resolution range 3.3–20 Å with R_{merge} = 10.8% (Table 1).

Structure determination and refinement. The crystal structure of the BAFF–BAFF-R complex was determined using molecular replacement (Table 1). The previously reported virus-like BAFF cage structure was used as a search probe[23]. The initial BAFF model was refined using CNS[41], and manually rebuilt using O[42]. Atoms related by 60-fold noncrystallographic symmetries (NCS) were tightly restrained throughout the refinement (weight = 300 kcal mol^{-1} Å^{-2}). NCS averaging greatly improved the quality of the electron density maps. After partial refinement of BAFF, a strong connected density was detected near the Arg265 residue of BAFF in an $F_o - F_c$ difference electron density map. The β-hairpin structure of the BAFF-R CRD was modeled in the density. The resulting BAFF–BAFF-R complex structure was further refined to the final *R*-factor of 23.9%, and R_{free} of 24.8%, calculated using the data in the resolution range 3.3–20 Å. The final atomic model includes 60 BAFF monomers (70,500 atoms), 60 BAFF-R monomers (11,220 atoms) and 40 magnesium ions (40 atoms). We assumed that the bound metal ions were magnesium ions, as proposed by Oren *et al*[22]. However, it is impossible to identify the bound metal ions unambiguously from current data exclusively. No water molecules were included in the model. The $F_o - F_c$ difference electron density map calculated using the refined structure shows a proteinlike density near the Tyr163 residue of BAFF. This is likely to be the electron density from the N-terminal arginine-rich region of BAFF-R. However, the structure of the residues in this region appeared to be unstable, and the quality of the map was not high enough for reliable modeling.

Binding assay. The BAFF-R extracellular domain (residues 1–63), the wild-type TACI full-length extracellular domain (residues 1–156), TACI CRD1 (residues 14–69) and TACI CRD2 (residues 67–111) were tagged with an Fc domain and expressed using a baculovirus expression system in Hi5 (Invitrogen) insect cells. The conserved aspartic acid and leucine residues of the DxL motifs were mutated to alanines in the mutant TACI domains. The mutant TACI domains were also expressed as Fc fusion proteins. The His_6-tagged BAFF and BAFF ΔDE mutant proteins were expressed in *Escherichia coli* and purified to homogeneity as earlier reported[23]. The culture media containing the secreted Fc-TACI or Fc-BAFF-R fusion proteins were incubated with protein A–Sepharose resins for 1 h at room temperature. Then, the resins were washed with a buffer containing 25 mM Tris at pH 6.0, 5% (v/v) glycerol, 0.25% (v/v) NP-40, 0.05 mM EDTA, 500 mM NaCl and 0.2 mM PMSF. A 2 μg sample of the purified BAFF and BAFF mutant proteins was then incubated with TACI- or BAFF-R-bound protein A–Sepharose resins. The final resins were washed and the bound proteins were subjected to SDS-PAGE. The resulting duplicate SDS-PAGE gels were visualized either by Coomassie Brilliant Blue staining or by immunoblot analysis using a polyclonal antibody specific for BAFF (Upstate Biotech). The latter approach was used because a protein contaminant runs at the same position as BAFF in the SDS-PAGE.

Coordinates. Coordinates and structure factors have been deposited in the Protein Data Bank (accession number 1OTZ).

Acknowledgments
We thank the staff of the Cornell High Energy Synchrotron Source (MacCHESS) and Spring-8 for help with data collection. This work was supported in part by the Molecular Medicine Research Group Program of the Ministry of Science (J.-O.L) and Technology and by a Korea Research Foundation Grant (H.L.).

Competing interests statement
The authors declare that they have no competing financial interests.

Received 14 February, 2003; accepted 4 April 2003.

1. Rolink, A.G. & Melchers, F. BAFFled B cells survive and thrive: roles of BAFF in B-cell development. *Curr. Opin. Immunol.* **14**, 266–275 (2002).
2. Mackay, F. & Mackay, C.R. The role of BAFF in B-cell maturation, T-cell activation and autoimmunity. *Trends Immunol.* **23**, 113–115 (2002).
3. Do, R.K. & Chen-Kiang, S. Mechanism of BLyS action in B cell immunity. *Cytokine Growth Factor Rev.* **13**, 19–25 (2002).
4. Tribouley, C. *et al*. Characterization of a new member of the TNF family expressed on antigen-presenting cells. *Biol. Chem.* **380**, 1443–1447 (1999).
5. Shu, H.B., Hu, W.H. & Johnson, H. TALL-1 is a novel member of the TNF family that is down-regulated by mitogens. *J. Leukoc. Biol.* **65**, 680–683 (1999).
6. Mukhopadhyay, A., Ni, J., Zhai, Y., Yu, G.L. & Aggarwal, B.B. Identification and characterization of a novel cytokine, THANK, a TNF homologue that activates apoptosis, nuclear factor-κB, and c-Jun NH_2-terminal kinase. *J. Biol. Chem.* **274**, 15978–15981 (1999).
7. Hu, S., Tamada, K., Ni, J., Vincenz, C. & Chen, L. Characterization of TNFRSF19, a novel member of the tumor necrosis factor receptor superfamily. *Genomics* **62**, 103–107 (1999).
8. Moore, P.A. *et al*. BLyS: member of the tumor necrosis factor family and B lymphocyte stimulator. *Science* **285**, 260–263 (1999).
9. Schneider, P. *et al*. BAFF, a novel ligand of the tumor necrosis factor family, stimulates B cell growth. *J. Exp. Med.* **189**, 1747–1756 (1999).
10. Gross, J.A. *et al*. TACI-Ig neutralizes molecules critical for B cell development and autoimmune disease. Impaired B cell maturation in mice lacking BLyS. *Immunity* **15**, 289–302 (2001).
11. Schiemann, B. *et al*. An essential role for BAFF in the normal development of B cells through a BCMA-independent pathway. *Science* **293**, 2111–2114 (2001).
12. Khare, S.D. *et al*. Severe B cell hyperplasia and autoimmune disease in TALL-1 transgenic mice. *Proc. Natl. Acad. Sci. USA* **97**, 3370–3375 (2000).
13. Mackay, F. *et al*. Mice transgenic for BAFF develop lymphocytic disorders along with autoimmune manifestations. *J. Exp. Med.* **190**, 1697–1710 (1999).
14. Groom, J. *et al*. Association of BAFF/BLyS overexpression and altered B cell differentiation with Sjogren's syndrome. *J. Clin. Invest.* **109**, 59–68 (2002).
15. Gross, J.A. *et al*. TACI and BCMA are receptors for a TNF homologue implicated in B-cell autoimmune disease. *Nature* **404**, 995–999 (2000).
16. Zhang, J. *et al*. Cutting edge: a role for B lymphocyte stimulator in systemic lupus erythematosus. *J. Immunol.* **166**, 6–10 (2001).
17. Cheema, G.S., Roschke, V., Hilbert, D.M. & Stohl, W. Elevated serum B lymphocyte stimulator levels in patients with systemic immune-based rheumatic diseases. *Arthritis Rheum.* **44**, 1313–1319 (2001).
18. Yan, M. *et al*. Identification of a receptor for BLyS demonstrates a crucial role in humoral immunity. *Nat. Immunol.* **1**, 37–41 (2000).
19. Xia, X.Z. *et al*. TACI is a TRAF-interacting receptor for TALL-1, a tumor necrosis factor family member involved in B cell regulation. *J. Exp. Med.* **192**, 137–143 (2000).
20. Wang, H. *et al*. TACI-ligand interactions are required for T cell activation and collagen-induced arthritis in mice. *Nat. Immunol.* **2**, 632–637 (2001).
21. Karpusas, M. *et al*. Crystal structure of extracellular human BAFF, a TNF family member that stimulates B lymphocytes. *J. Mol. Biol.* **315**, 1145–1154 (2002).
22. Oren, D.A. *et al*. Structural basis of BLyS receptor recognition. *Nat. Struct. Biol.* **9**, 288–292 (2002).
23. Liu, Y. *et al*. Crystal structure of sTALL-1 reveals a virus-like assembly of TNF family ligands. *Cell* **108**, 383–394 (2002).
24. Yan, M. *et al*. Identification of a novel receptor for B lymphocyte stimulator that is mutated in a mouse strain with severe B cell deficiency. *Curr. Biol.* **11**, 1547–1552 (2001).
25. Thompson, J.S. *et al*. BAFF-R, a newly identified TNF receptor that specifically interacts with BAFF. *Science* **293**, 2108–2111 (2001).
26. Thompson, J.S. *et al*. BAFF binds to the tumor necrosis factor receptor-like molecule B cell maturation antigen and is important for maintaining the peripheral B cell population. *J. Exp. Med.* **192**, 129–135 (2000).
27. Marsters, S.A. *et al*. Interaction of the TNF homologues BLyS and APRIL with the TNF receptor homologues BCMA and TACI. *Curr. Biol.* **10**, 785–788 (2000).
28. Seshasayee, D. *et al*. Loss of TACI causes fatal lymphoproliferation and autoimmunity, establishing TACI as an inhibitory BLyS receptor. *Immunity* **18**, 279–288 (2003).
29. von Bulow, G.U., van Deursen, J.M. & Bram, R.J. Regulation of the T-independent humoral response by TACI. *Immunity* **14**, 573–582 (2001).
30. Yan, M. *et al*. Activation and accumulation of B cells in TACI-deficient mice. *Nat. Immunol.* **2**, 638–643 (2001).
31. Locksley, R.M., Killeen, N. & Lenardo, M.J. The TNF and TNF receptor superfamilies: integrating mammalian biology. *Cell* **104**, 487–501 (2001).
32. Bodmer, J.L., Schneider, P. & Tschopp, J. The molecular architecture of the TNF superfamily. *Trends Biochem. Sci.* **27**, 19–26 (2002).
33. Naismith, J.H., Devine, T.Q., Kohno, T. & Sprang, S.R. Structures of the extracellular domain of the type I tumor necrosis factor receptor. *Structure* **4**, 1251–1262 (1996).
34. Naismith, J.H. & Sprang, S.R. Modularity in the TNF-receptor family. *Trends Biochem. Sci.* **23**, 74–79 (1998).
35. Mongkolsapaya, J. *et al*. Structure of the TRAIL-DR5 complex reveals mechanisms conferring specificity in apoptotic initiation. *Nat. Struct. Biol.* **6**, 1048–1053 (1999).
36. Hymowitz, S.G. *et al*. Triggering cell death: the crystal structure of Apo2L/TRAIL in a complex with death receptor 5. *Mol. Cell* **4**, 563–571 (1999).
37. Banner, D.W. *et al*. Crystal structure of the soluble human 55 kD TNF receptor-human TNF β-complex: implications for TNF receptor activation. *Cell* **73**, 431–445 (1993).
38. Kayagaki, N. *et al*. BAFF/BLyS receptor 3 binds the B cell survival factor BAFF ligand through a discrete surface loop and promotes processing of NF-κB2. *Immunity* **17**, 515–524 (2002).
39. Madry, C. *et al*. The characterization of murine BCMA gene defines it as a new member of the tumor necrosis factor receptor superfamily. *Int. Immunol.* **10**, 1693–1702 (1998).
40. Otwinowski, Z. & Minor, W. Processing of X-ray diffraction data collected in oscillation mode. *Methods Enzymol.* **276**, 307–326 (1997).
41. Brunger, A.T. *et al*. Crystallography & NMR system: a new software suite for macromolecular structure determination. *Acta Crystallogr. A* **54**, 905–921 (1998).
42. Jones, T.A., Zou, J.Y., Cowan, S.W. & Kjeldgaard, M. Improved methods for binding protein models in electron density maps and the location of errors in these models. *Acta. Crystallogr. A* **47**, 110–119 (1991).
43. Vriend, G. WHAT IF: a molecular modeling and drug design program. *J. Mol. Graph.* **8**, 52–56 (1990).